Available online at www.sciencedirect.com

ScienceDirect

Journal of Computational and Applied Mathematics 210 (2007) 106–115

JOURNAL OF COMPUTATIONAL AND APPLIED MATHEMATICS

www.elsevier.com/locate/cam

Approximation of functionally graded plates with non-conforming finite elements

Claudia Chinosi[a], Lucia Della Croce[b,*]

[a] *Dipartimento di Scienze e Tecnologie Avanzate Università del Piemonte Orientale, Alessandria, Italy*
[b] *Dipartimento di Matematica Università di Pavia, Via Ferrata 1, 27100 Pavia, Italy*

Received 12 July 2005; received in revised form 24 February 2006

Abstract

In this paper rectangular plates made of functionally graded materials (FGMs) are studied. A two-constituent material distribution through the thickness is considered, varying with a simple power rule of mixture. The equations governing the FGM plates are determined using a variational formulation arising from the Reissner–Mindlin theory. To approximate the problem a simple locking-free Discontinuous Galerkin finite element of non-conforming type is used, choosing a piecewise linear non-conforming approximation for both rotations and transversal displacement. Several numerical simulations are carried out in order to show the capability of the proposed element to capture the properties of plates of various gradings, subjected to thermo-mechanical loads.

MSC: 74S05; 74K20; 74E30

Keywords: Functionally graded plates; Reissner–Mindlin plates; Non-conforming finite element methods

1. Introduction

The concept of functionally graded materials (FGMs) was proposed in 1984 by the Japanese school of material science, as novel materials with thermal barrier or heat shielding properties (see e.g., [14,21]). Successively much research activities have followed both within Japan and all over the world. FGMs are composite materials that are microscopically non-homogeneous but at macro level, the mechanical properties vary continuously from one surface to another by smoothly varying the volume fractions of the material constituents. A considerable part of studies on FGMs is largely devoted to thermal stress analysis and fracture analysis in plates and shells [23,13]. During the years theoretical formulations and finite element models have been presented to deal with either type of problems. Remarkable contributions in thermal stress analysis include [22,17,19] and a series of pioneering papers of the Japanese school for which reference is made to [18] among the others. Basic and methodological considerations on fracture mechanics for FGMs may be found for instance in [11,12]. Several authors (see e.g., [7,18,17]) have used either a first-order or a third-order shear deformation plate theory coupled with the finite element method to analyze the deformations of FGM plates. Here we study a thermo-mechanical problem and use the Reissner–Mindlin plate theory [20,16] to analyze the static response of plates of different material grading. Regarding the numerical approximation, we follow the variational

* Corresponding author.
E-mail address: lucia.dellacroce@unipv.it (L. Della Croce).

0377-0427/$ - see front matter © 2006 Elsevier B.V. All rights reserved.
doi:10.1016/j.cam.2006.10.078

approach already introduced in [10] and, as an alternative to the more classical finite element schemes employed, we apply a Discontinuous Galerkin method. In recent times there has been a considerable interest in the extension of Discontinuous Galerkin techniques to the treatment of elliptic problems for various applications (see e.g., [1] and the references therein). In particular, for Reissner–Mindlin plates, a family of locking-free elements have been introduced in [2]. Starting from the basic ingredients indicated there, simple DG-based finite elements of non-conforming type have been presented in [6,9]. The aim of our contribution is to assess the performance of a non-conforming finite element approximation of the latter type, to capture the properties of plates of various gradings, subjected to thermo-mechanical loads. The element uses piecewise linear non-conforming approximation for both rotations and transversal displacement. Results of physical interest are proposed concerning thermoelastic analysis of a moderately thin plate made of two constituents. The paper is organized as follows. Section 2 presents basic governing equations of the problem. Section 3 gives the mixed formulation of the problem and details its non-conforming approximation. Several numericals results in accordance with the expected physical behavior are reported in Section 4.

2. Governing equations

2.1. Functionally graded materials law and thermal analysis

We consider a plate of thickness t made of two-constituent material distribution such as ceramic and metal, varying in the thickness direction. To obtain the effective properties of the graded plate a simple rule of mixture is adopted, i.e., a power law of type

$$V(z) = (V_{\mathrm{t}} - V_{\mathrm{b}})\left(\frac{2z+t}{2t}\right)^n + V_{\mathrm{b}}, \tag{1}$$

where V denotes a generic material property, V_{t} and V_{b} are the corresponding values at the top and bottom faces of the plate, z is the thickness coordinate ($-t/2 \leqslant z \leqslant t/2$) and $n \geqslant 0$ is the volume fraction exponent.

A homogeneous plate made of the top-material only (ceramic) is retrieved for $n = 0$, while the content of bottom-material (metal) in the plate increases as the value of n increases. Here we assume that the elastic and thermal properties of the material vary according to Eq. (1). Since the functionally graded plates are primarily used when large temperature gradients occur, our focus is to analyze the influence of the temperature field on them. We assume that the temperature is constant at the ceramic and metal surfaces and it depends on the z coordinate only. The temperature distribution along the thickness can be obtained by solving the one-dimensional steady state heat transfer equation:

$$-\frac{\mathrm{d}}{\mathrm{d}z}\left(\lambda(z)\frac{\mathrm{d}T}{\mathrm{d}z}\right) = 0 \tag{2}$$

with the thermal boundary conditions

$$T = T_{\mathrm{t}} \ \text{ at } z = t/2, \quad T = T_{\mathrm{b}} \ \text{ at } z = -t/2.$$

The solution of Eq. (2) may be evaluated exactly and it reads

$$T(z) = T_{\mathrm{t}} - \frac{T_{\mathrm{t}} - T_{\mathrm{b}}}{\int_{-t/2}^{t/2}(\mathrm{d}z/\lambda(z))}\int_z^{t/2}\frac{\mathrm{d}\xi}{\lambda(\xi)}, \tag{3}$$

where the thermal conductivity $\lambda(z)$ varies according to power law distribution (1). When λ does not depend on z (thermally homogeneous plate), the temperature distribution is linear through the thickness. Excursions from the linear distribution are obtained by changing the volume fraction index n, as shown in Fig. 1. The thermal effects are classically introduced at the constitutive level, as we will describe in the next section.

2.2. The Reissner–Mindlin model

The equations of motion are based on a suitable extension of the classical Reissner–Mindlin model. This theory describes accurately the global behavior of graded material plates, characterized by non-negligible shear deformation.

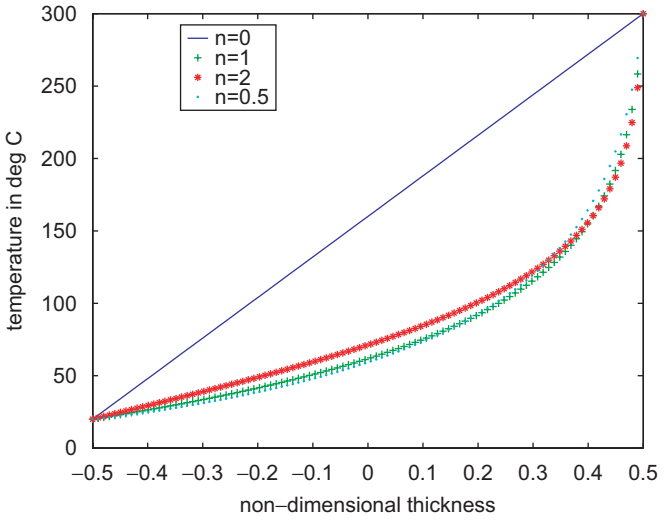

Fig. 1. Temperature vs plate thickness for various values of n.

An orthogonal Cartesian frame is introduced, the (x, y) plane being the undeformed midplane of the plate. The unknowns of the Reissner–Mindlin model are the normal displacement w and the vector $\boldsymbol{\theta} = [\theta_x, \theta_y]$ of the rotations of the normal to the undeformed middle surface in the x–z and y–z planes, respectively. The so-called in-plane displacements u, v and the normal displacement w in this model have the form

$$u(x, y, z) = -z\theta_x(x, y), \quad v(x, y, z) = -z\theta_y(x, y), \quad w(x, y, z) = w(x, y). \tag{4}$$

Let ε be the usual symmetric gradient operator, giving

$$\varepsilon(\boldsymbol{\theta}) = [\theta_{x,x}, \theta_{y,y}, \theta_{x,y} + \theta_{y,x}]^{\mathrm{T}}. \tag{5}$$

The three components of in-plane mechanical strain vector $\boldsymbol{\epsilon}$ are defined as

$$\boldsymbol{\epsilon} = -z\varepsilon(\boldsymbol{\theta}). \tag{6}$$

When the plate is subjected to a given temperature distribution T with a thermal coefficient of expansion $\alpha(z)$, the thermal strain vector $\boldsymbol{\epsilon}^{\mathrm{th}}$ must be considered:

$$\boldsymbol{\epsilon}^{\mathrm{th}} = [\alpha(z)(T(z) - T_0), \alpha(z)(T(z) - T_0), 0]^{\mathrm{T}}, \tag{7}$$

where T_0 is the temperature corresponding to the stress-free state. The vector of transverse shear $\boldsymbol{\gamma}$ is constant through the thickness and it is defined as

$$\boldsymbol{\gamma} = \nabla w - \boldsymbol{\theta}. \tag{8}$$

In-plane and out-of-plane stress-strain constitutive law depends on the material distribution and on the thermal effects. The governing equations cease to be standard in that the resulting plate coefficients depend on the selected grading profile. We can write

$$\boldsymbol{\sigma} = B(z)(\boldsymbol{\epsilon} - \boldsymbol{\epsilon}^{\mathrm{th}}), \quad \boldsymbol{\tau} = S(z)\boldsymbol{\gamma}, \tag{9}$$

where $\boldsymbol{\sigma} = [\sigma_x, \sigma_y, \sigma_{xy}]^{\mathrm{T}}$ and $\boldsymbol{\tau} = [\tau_x, \tau_y]^{\mathrm{T}}$ are the total in-plane and shear stresses. The grading matrices $B(z)$ and $S(z)$ are defined as

$$B(z) = \frac{E(z)}{1 - \nu^2} \begin{bmatrix} 1 & \nu & 0 \\ \nu & 1 & 0 \\ 0 & 0 & \dfrac{1 - \nu}{2} \end{bmatrix}, \quad S(z) = \frac{E(z)}{1 - \nu^2} \begin{bmatrix} \dfrac{1 - \nu}{2} & 0 \\ 0 & \dfrac{1 - \nu}{2} \end{bmatrix}. \tag{10}$$

The Young modulus of elasticity $E(z)$ and the thermal coefficient $\alpha(z)$ change through the thickness z according to law (1), while Poisson's ratio v is assumed to be constant. Let us denote with $V = \Omega \times (-t/2, t/2)$ the region in $\mathbf{R}^3$ occupied by the undeformed graded elastic plate. We assume that the mechanical load acting on the plate is normal to its surface, i.e., $\mathbf{q} = [0, 0, q]^{\mathrm{T}}$ and that the deflections are small in comparison with the thickness of the plate. In the Reissner–Mindlin model the total potential energy can be written as

$$\Pi(\theta_x, \theta_y, w) = \frac{1}{2}\int_V \boldsymbol{\sigma}\cdot\boldsymbol{\epsilon}\,\mathrm{d}V + \frac{k}{2}\int_V \boldsymbol{\tau}\cdot\boldsymbol{\gamma}\,\mathrm{d}V - \int_V q w\,\mathrm{d}V \tag{11}$$

where k is the shear correction factor. After integration through the thickness, we obtain

$$\Pi(\theta_x, \theta_y, w) = \frac{1}{2}\int_\Omega (\varepsilon(\boldsymbol{\theta}))^{\mathrm{T}} D\varepsilon(\boldsymbol{\theta})\,\mathrm{d}x\,\mathrm{d}y + \frac{1}{2}\int_\Omega \mathbf{m}^{\mathrm{th}}\cdot\varepsilon(\boldsymbol{\theta})\,\mathrm{d}x\,\mathrm{d}y + \frac{k}{2}\int_\Omega \boldsymbol{\gamma}^{\mathrm{T}} Q\boldsymbol{\gamma}\,\mathrm{d}x\,\mathrm{d}y - \int_\Omega pw\,\mathrm{d}x\,\mathrm{d}y. \tag{12}$$

In the above relation we have introduced the elasticity matrices

$$D = \int_{-t/2}^{t/2} B(z)z^2\,\mathrm{d}z, \quad Q = \int_{-t/2}^{t/2} S(z)\,\mathrm{d}z, \tag{13}$$

the vector of the thermal moments

$$\mathbf{m}^{\mathrm{th}} = \int_{-t/2}^{t/2} B(z)\boldsymbol{\epsilon}^{\mathrm{th}} z\,\mathrm{d}z = \frac{1}{1-v}\begin{bmatrix} \int_{-t/2}^{t/2}\alpha(z)E(z)(T(z)-T_0)z\,\mathrm{d}z \\ \int_{-t/2}^{t/2}\alpha(z)E(z)(T(z)-T_0)z\,\mathrm{d}z \\ 0 \end{bmatrix} \tag{14}$$

and the mechanical load p per unit area. Stationarity of the total potential energy Π is used to derive the variational formulation of the functionally graded plate needed for the development of our finite element approach. Let $\boldsymbol{\Theta}$ and W be the spaces of admissible deformations, the classical variational formulation of the minimum problem related to the functional (12) becomes

$$\begin{cases} \text{Find}(\boldsymbol{\theta}, w) \in \boldsymbol{\Theta}\times W : \\ \int_\Omega (\varepsilon(\boldsymbol{\theta}))^{\mathrm{T}} D\varepsilon(\boldsymbol{\eta})\,\mathrm{d}x\,\mathrm{d}y + s\int_\Omega (\nabla w - \boldsymbol{\theta})\cdot(\nabla v - \boldsymbol{\eta})\,\mathrm{d}x\,\mathrm{d}y \\ \quad = \int_\Omega pv\,\mathrm{d}x\,\mathrm{d}y - \frac{1}{2}\int_\Omega \mathbf{m}^{\mathrm{th}}\cdot\varepsilon(\boldsymbol{\eta})\,\mathrm{d}x\,\mathrm{d}y \quad \forall(\boldsymbol{\eta}, v)\in\boldsymbol{\Theta}\times W, \end{cases} \tag{15}$$

where the shear modulus s is related to matrix Q ($Q = (s/k)I$, I identity matrix):

$$s = \frac{k}{2(1+v)}\int_{-t/2}^{t/2} E(z)\,\mathrm{d}z.$$

3. The mixed formulation and the non-conforming finite element

It is well known that a straightforward discretization of the problem (15) by means of finite elements typically suffers from the so-called shear-locking phenomenon. A common way to overcome this lack of convergence is to introduce a mixed formulation. It is usually derived by introducing the shear force

$$\boldsymbol{\xi} = s(\nabla w - \boldsymbol{\theta})$$

as an independent variable. Suppose that Ω is a convex with regular boundary $\partial\Omega$ and that the plate is simply supported. The mixed variational formulation of the problem (15) can be written as

$$\begin{cases} \text{Find}(\boldsymbol{\theta}, w, \boldsymbol{\xi}) \in \boldsymbol{\Theta}\times W\times \mathbf{L}^2(\Omega) : \\ a(\boldsymbol{\theta}, \boldsymbol{\eta}) + (\nabla v - \boldsymbol{\eta}, \boldsymbol{\xi}) = (p, v) - \frac{1}{2}(\mathbf{m}^{\mathrm{th}}, \varepsilon(\boldsymbol{\eta})) \quad \forall\,(\boldsymbol{\eta}, v)\in\boldsymbol{\Theta}\times W, \\ (\nabla w - \boldsymbol{\theta}, \boldsymbol{\gamma}) - s^{-1}(\boldsymbol{\xi}, \boldsymbol{\gamma}) = 0 \qquad\qquad \forall\,\boldsymbol{\gamma}\in\mathbf{L}^2(\Omega), \end{cases} \tag{16}$$

where $p \in L^2(\Omega)$, $(\cdot,\cdot)$ is the inner-product in $L^2(\Omega)$ (or in $\mathbf{L}^2(\Omega)$) and

$$\boldsymbol{\Theta} = \{\boldsymbol{\eta} \in \mathbf{H}^1(\Omega), \boldsymbol{\eta}\cdot\boldsymbol{\delta} = 0 \text{ on } \partial\Omega\},$$

$$W = H_0^1(\Omega),$$

$$a(\boldsymbol{\theta},\boldsymbol{\eta}) := \int_\Omega \varepsilon(\boldsymbol{\theta})^{\mathrm{T}} D\varepsilon(\boldsymbol{\eta})\ \mathrm{d}x\,\mathrm{d}y. \tag{17}$$

In the definition of $\boldsymbol{\Theta}$, $\boldsymbol{\delta}$ denotes the counterclockwise unit tangent vector to the boundary $\partial\Omega$. The weak formulation (16) takes the form of the classical mixed Reissner–Mindlin plate problem. Under our regularity assumptions, it is easy to prove (see [5] for instance) the existence and the uniqueness of the solution. The discretization of mixed formulation (16) requires the choice of suitable finite element spaces in order to achieve stability and uniform convergence of the discrete solution. A lot of stable and convergent mixed methods have been presented in the latest years (see for instance [3,4,2] and the references therein). Among them we mention the Discontinuous Galerkin based finite elements, recently extended to the treatment of the Reissner–Mindlin plates. These elements seem to be favorable to study problems with discontinuous solutions, that for instance arise in applications involving severe thermal gradients. The FGM plates are ideal candidates to treat situations where large temperature changes are encountered. Hence we will consider a non-conforming finite element based on the Discontinuous Galerkin approach to determine the behavior of FGMs subjected to a through-the-thickness temperature gradient.

We now introduce the non-conforming finite element approximation of problem (16), following the approach detailed in [6]. Let $\mathscr{T}_h$ be a regular decomposition of Ω into triangular elements K, and let us set $H^1(\mathscr{T}_h) := \prod_{K\in\mathscr{T}_h} H^1(K)$. Let $\mathscr{E}_h$ denote the set of all the edges in $\mathscr{T}_h$, and $\mathscr{E}_h^{\mathrm{in}}$ the set of internal edges. Let e be an internal edge of $\mathscr{T}_h$, shared by two elements K^+ and K^-, and let φ denote a function in $H^1(\mathscr{T}_h)$, or a vector in $\mathbf{H}^1(\mathscr{T}_h)$. We define the typical operators arising in discontinuous formulations, i.e., average and jumps. We have as usual for the average

$$\{\varphi\} = \frac{\varphi^+ + \varphi^-}{2} \quad \forall e \in \mathscr{E}_h^{\mathrm{in}}, \tag{18}$$

while for the definition of jump operators we refer to [2]: let $\varphi \in H^1(\mathscr{T}_h)$ be a scalar function, its jump is

$$[\varphi] = \varphi^+\mathbf{n}^+ + \varphi^-\mathbf{n}^- \quad \forall e \in \mathscr{E}_h^{\mathrm{in}}, \tag{19}$$

let $\boldsymbol{\varphi} \in \mathbf{H}^1(\mathscr{T}_h)$ be a vector, its jump is given by

$$[\boldsymbol{\varphi}] = (\boldsymbol{\varphi}^+ \otimes \mathbf{n}^+)_{\mathrm{S}} + (\boldsymbol{\varphi}^- \otimes \mathbf{n}^-)_{\mathrm{S}} \quad \forall e \in \mathscr{E}_h^{\mathrm{in}}, \tag{20}$$

where $(\boldsymbol{\varphi}\otimes\mathbf{n})_{\mathrm{S}}$ denotes the symmetric part of the tensor product, and $\mathbf{n}^+$ (resp. $\mathbf{n}^-$) is the outward unit normal to ∂K^+ (resp. to ∂K^-). On the boundary edges we define jumps of scalars as $[\varphi] = \varphi\mathbf{n}$, and jumps of vectors as $[\boldsymbol{\varphi}] = (\boldsymbol{\varphi}\otimes\mathbf{n})_{\mathrm{S}}$, where $\mathbf{n}$ is the outward unit normal to $\partial\Omega$. We also define averages of vectors and tensors as $\{\boldsymbol{\varphi}\} = \boldsymbol{\varphi}$.

We introduce a *low-order* polynomial approximation, already detailed in [15,9]. Here it has been proved that this element has an optimal approximation order in the H^1-broken and L^2 norm, respectively. The element is based on the use of non-conforming piecewise linear functions for both rotations and transversal displacement. It is characterized by the following spaces:

$$\boldsymbol{\Theta}_h = \left\{\boldsymbol{\eta} : \boldsymbol{\eta}_{|K} \in (P_1(K))^2,\ \int_e [\boldsymbol{\eta}]\,\mathrm{d}s = 0\ \forall e \in \mathscr{E}_h^{\mathrm{in}},\ \int_e \boldsymbol{\eta}\cdot\boldsymbol{\delta}\,\mathrm{d}s = 0,\ \forall e \in \partial\Omega\right\} \subset \mathbf{H}^1(\mathscr{T}_h), \tag{21}$$

$$W_h = \left\{v : v_{|K} \in P_1(K),\ \int_e [v]\,\mathrm{d}s = 0\ \forall e \in \mathscr{E}_h\right\} \subset H^1(\mathscr{T}_h), \tag{22}$$

$$\boldsymbol{\Gamma}_h = \left\{\boldsymbol{\gamma} : \boldsymbol{\gamma}_{|K} \in (P_0(K))^2\right\} \subset \mathbf{L}^2(\Omega). \tag{23}$$

In Fig. 2 we show the proposed finite element, together with its degrees of freedom. We note the simplicity of the element, due to the low degree of polynomials and the fact that the original unknowns $(\boldsymbol{\theta}, w)$ share the same nodes.

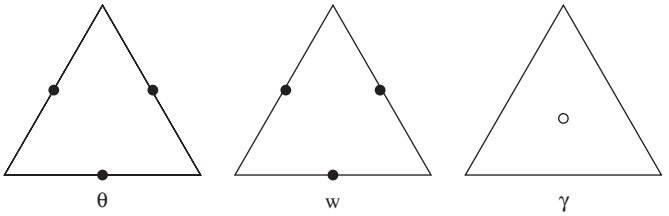

Fig. 2. The non-conforming element.

With the previous choices the discretization of problem (16) can be written as

$$\begin{cases} \text{Find}(\boldsymbol{\theta}_h, w_h, \boldsymbol{\xi}_h) \in \boldsymbol{\Theta}_h \times W_h \times \boldsymbol{\Gamma}_h \\ a_h(\boldsymbol{\theta}_h, \boldsymbol{\eta}_h) + (\nabla_h v_h - \mathbf{R}_h \boldsymbol{\eta}_h, \boldsymbol{\xi}_h) = (p, v_h) - \frac{1}{2}(\mathbf{m}^{\text{th}}, \varepsilon_h(\boldsymbol{\eta}_h)) \quad \forall (\boldsymbol{\eta}_h, v_h) \in \boldsymbol{\Theta}_h \times W_h \\ (\nabla_h w_h - \mathbf{R}_h \boldsymbol{\theta}_h, \boldsymbol{\gamma}_h) - s^{-1}(\boldsymbol{\xi}_h, \boldsymbol{\gamma}_h) = 0 \quad \forall \boldsymbol{\gamma}_h \in \boldsymbol{\Gamma}_h. \end{cases} \tag{24}$$

Above, ∇_h and ε_h denote the gradient and symmetric gradient operators element by element and $\mathbf{R}_h : \mathbf{H}^1(\mathscr{T}_h) \to \boldsymbol{\Gamma}_h$ is the L^2-projection operator onto the piecewise constant functions. The bilinear form $a_h(\cdot\,,\cdot)$ is defined by

$$a_h(\boldsymbol{\theta}, \boldsymbol{\eta}) := \sum_{K \in \mathscr{T}_h} \int_K (\varepsilon(\boldsymbol{\theta}))^{\mathrm{T}} D\varepsilon(\boldsymbol{\eta})\, \mathrm{d}x\, \mathrm{d}y + p_\Theta(\boldsymbol{\theta}, \boldsymbol{\eta}), \tag{25}$$

where p_Θ is a penalty term

$$p_\Theta(\boldsymbol{\theta}, \boldsymbol{\eta}) := \sum_{e \in \mathscr{E}_h} \frac{\kappa_{\mathrm{e}}}{|e|} \int_e [\boldsymbol{\theta}] : [\boldsymbol{\eta}]\, \mathrm{d}s \quad (|e| := \text{length of the edge } e) \tag{26}$$

introduced in order to achieve the coercivity of the bilinear form (25) on $\boldsymbol{\Theta}_h$. In (26) κ_{e} is a positive constant having the same physical dimension as D; for instance one could take $\kappa_{\mathrm{e}} = \text{euclidean norm of } D$. Dropping it or taking it *too small* may cause a loss of stability for the scheme (see [8]).

4. Numerical results

In this section we present several numerical simulations, in order to assess the behavior of functionally graded plates subjected to mechanical and thermal loads when discontinuous finite elements are used. To this aim we will consider a simply supported square plate of side $a = 0.2$ m and thickness $t = 0.01$ m. The plate is made by a ceramic material at the top, a metallic material at the bottom and law (1), with $n = 0, 0.5, 1, 2$ is used for the through-the-thickness variation. The plate is loaded by a uniformly distributed mechanical normal load on the top surface and a thermal field is also assumed, with $T_0 = 0\,^\circ$C. The material parameters are summarized in Table 1 (left). As usual, the results are presented in terms of non-dimensionalized parameters, detailed in Table 1 (right). All the results are obtained choosing $\kappa_{\mathrm{e}} = \text{euclidean norm of } D$. We have analyzed the behavior of the plate, when subjected to increasing mechanical load. At first, we assume to have only a mechanical load and we consider a uniform $15 \times 15 \times 2$ triangulation. In Fig. 3 (left) the central deflection $\overline{w}$ with respect to mechanical loads P for different values of exponent n is reported. We observe that the deflection of the metallic plate has the largest magnitude, while the deflection of the ceramic plate keeps the smallest one. All the plates of intermediate properties assume corresponding intermediate deflections. In Fig. 3 (right) the variation of the center deflection in the presence of the temperature field is presented, versus increasing mechanical loads. In this case the behavior of graded plates is not intermediate to the metal and ceramic plates. The center deflections of the homogeneous plates are higher than those of the graded plates and initially all of them are positive. As the temperature effect reduces with increasing mechanical loads, the deflections become negative and tend toward a behavior similar to the case of pure pressure loads. Moreover, we note that the deflections of the intermediate plates under temperature field are close to each other, according to temperature profiles shown in Fig 1. We can observe that the results obtained here are in perfect agreement with those presented in [18,10]. To understand better the response

Table 1
Material properties

	Aluminum	Zirconia	Parameter scaling	
E	70 GPa	151 GPa	Deflection	$\overline{w} = w/t$
ν	0.3	0.3	Load	$P = (pa^4)/(E_b t^4)$
λ	204 W/mK	2.09 W/mK	z-Coordinate	$\overline{z} = z/t$
α	23×10^{-6}/C	10×10^{-6}/C	Shear stress	$\overline{\tau}_x = \tau_x t/(pa)$
T	20 °C	300 °C	Axial stress	$\overline{\sigma}_x = \sigma_x t^2/(pa^2)$

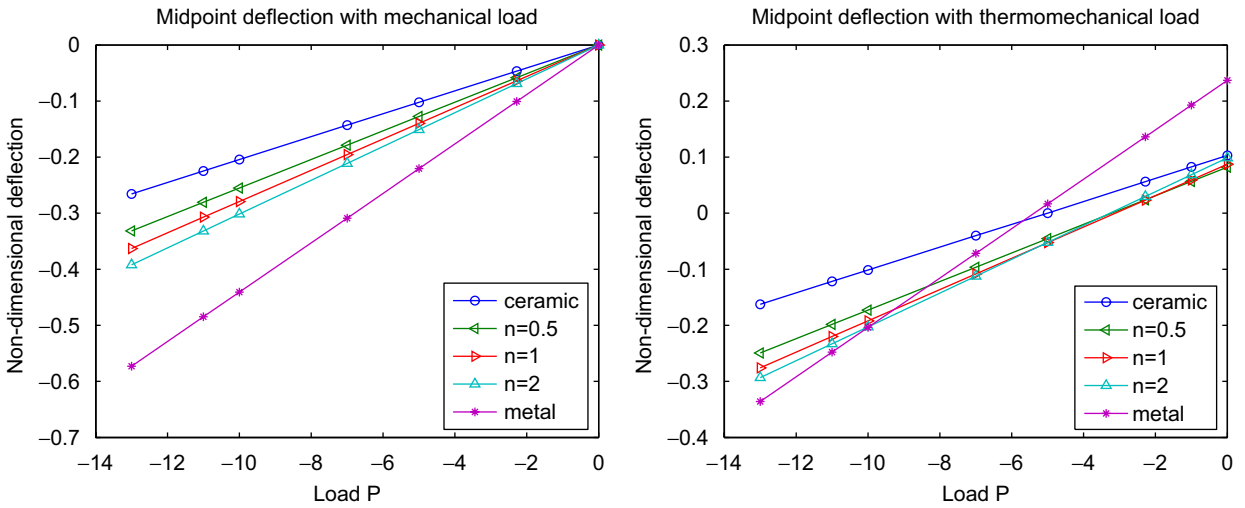

Fig. 3. Midpoint deflection versus load P (on the left mechanical load, on the right thermo-mechanical load).

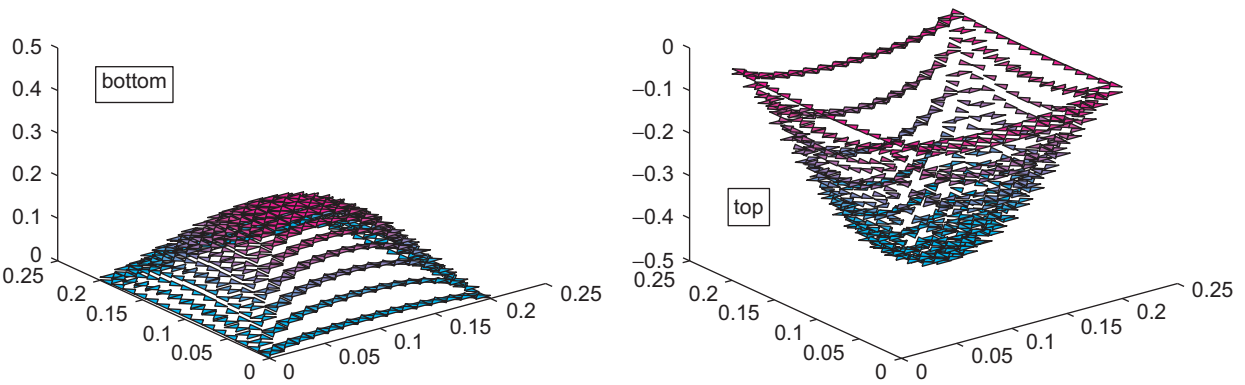

Fig. 4. Graphs of axial stress with mechanical load ($n = 2$).

of FGM plates, it is convenient to analyze the stresses. We consider a fixed mechanical load $p = -10^6\,\mathrm{N/m^2}$ applied on the top surface and we study the through-the-thickness variation of the axial and shear stresses for different values of the exponent n. We consider a uniform *criss-cross* $15 \times 15 \times 4$ triangulation. As it appears in Fig. 4, where the bi-dimensional graphs of $\overline{\sigma}_x$ at the bottom and the top of the plate corresponding to $n = 2.0$ are plotted, the axial stresses are compressive at the top surface and tensile at the bottom surface and they yield the maximum at the center of the surface. Fig. 5 (left) depicts the through-the-thickness axial stress evaluated at points on the centroidal axis. It shows that the FGM plate corresponding to $n = 2.0$ reaches the maximum tensile stress at the top surface while

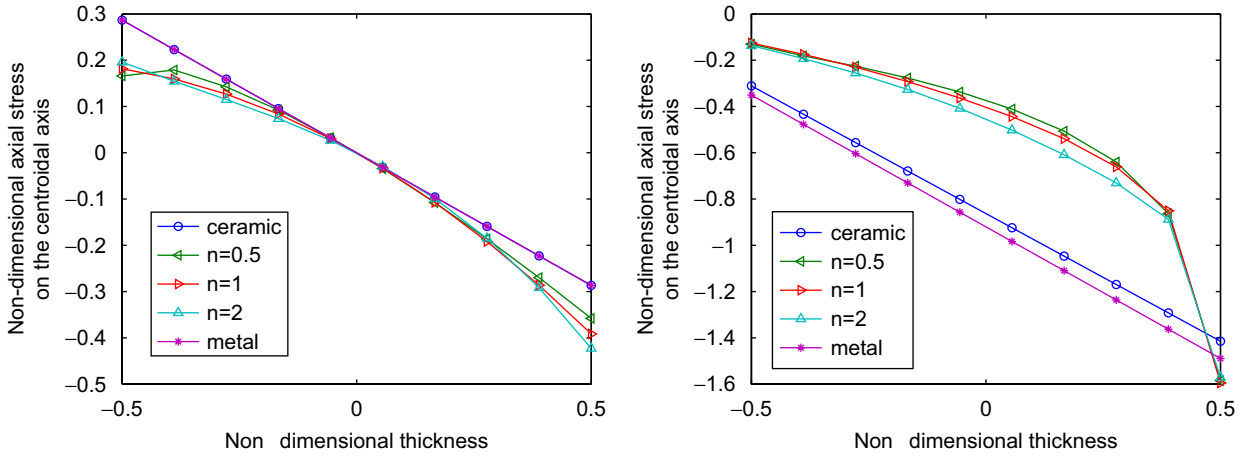

Fig. 5. Axial stress with (on the left) mechanical load, (on the right) thermo-mechanical load.

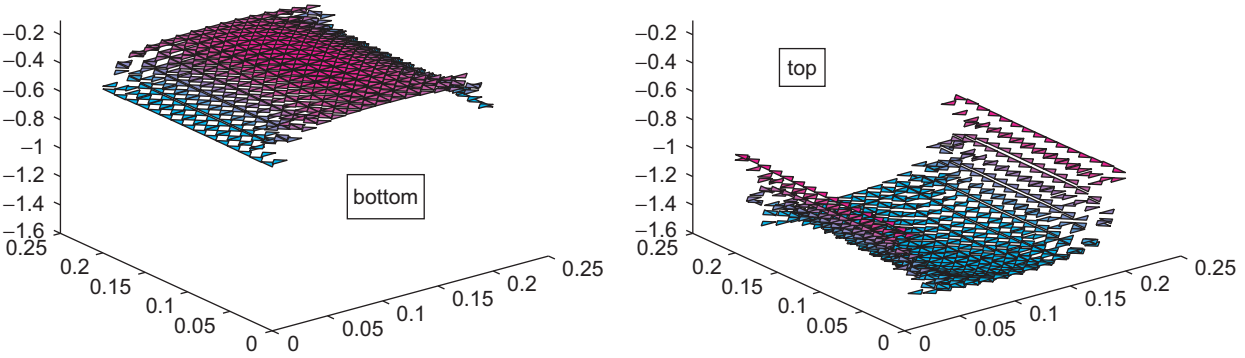

Fig. 6. Graphs of axial stress with thermo-mechanical load ($n = 2$).

the metallic and ceramic plates reach the maximum tensile stress at the bottom surface. The results obtained when a temperature field is applied are shown in Figs. 5 (right) and 6. The latter displays that the stresses reach the maximum at the center of the surface. So, also in this case, we evaluated the through-the-thickness axial stresses at points on the centroidal axis. We observe in Fig. 5 that the stresses are compressive both at the top and at the bottom surface. The profiles of the compressive stress for the graded plates are close to each other and their magnitude is less than the one of the homogeneous plates. All the results are in agreement with those presented in [18,10]. Our simulations have been devoted to the computation of shear stresses, whose approximation directly allows from the feature of the mixed formulation used. Indeed, usually adopting a mixed approach the shear force is introduced as an independent variable, so its evaluation is straightforward. We report in Fig. 7 the shear stress $\overline{\tau}_x$ at the bottom and at the top surface for $n = 2$ in the case of mechanical load only ($p = -10^6\,\mathrm{N/m^2}$). One can observe that the shear stress is antisymmetric with respect to the central axis and it reaches the maximum value near the boundary. In Fig. 8 (left) we show the through-the-thickness shear stress evaluated near the maximum point. As expected, the behavior of the shear stress for homogeneous plates is constant, unlike when the volume fraction exponent varies. A similar behavior is observed in the case of thermo-mechanical load, as shown in Fig. 8 (right). The likeness is due to the fact that the shear stress does not depend explicitly on the temperature field.

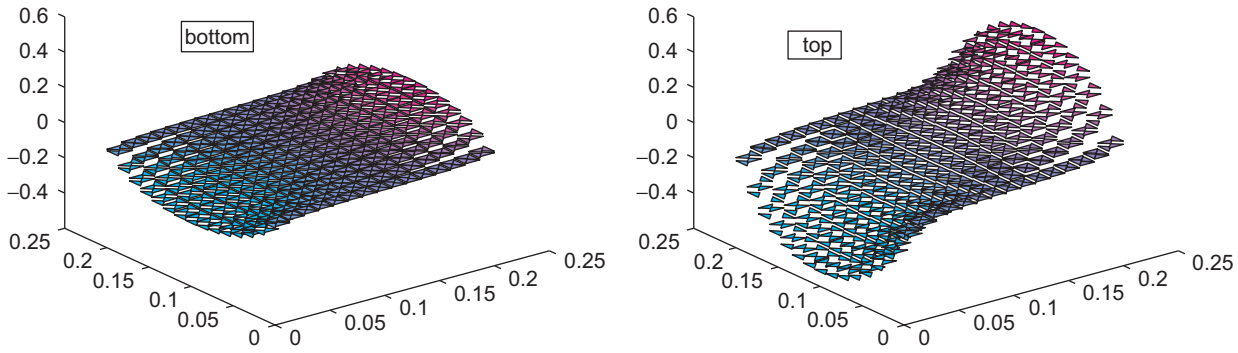

Fig. 7. Graphs of shear stress with mechanical load ($n = 2$).

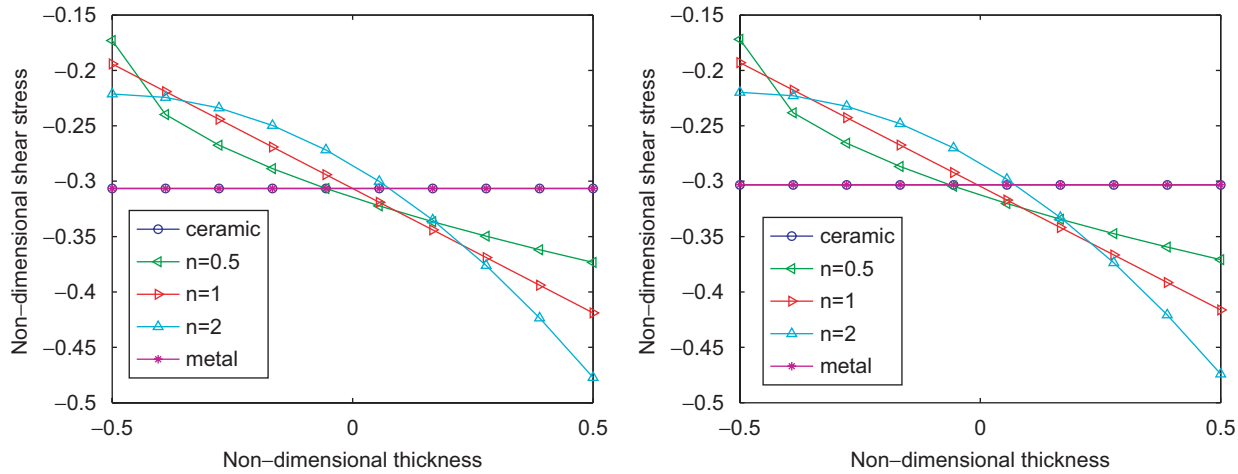

Fig. 8. Shear stress with (on the left) mechanical load, (on the right) thermo-mechanical load.

5. Conclusions

A simple locking-free Discontinuous Galerkin finite element of non-conforming type has been presented to analyze the Reissner–Mindlin functionally graded plates. The static thermoelastic response of plates with various gradings has been assessed and compared to the one of single-constituent homogeneous plates. The deflections and the axial stresses have been computed under mechanical loading and thermal loading. The mixed formulation adopted has allowed the straightforward computation of the shear stresses. The numerical simulations have shown that the element performs well and the results are in agreement with those obtained using standard finite elements. A further comparison in terms of accuracy and computational cost with other approaches could be made later. The peculiar features of the discontinuous approach suggest that the element extension to fracture analysis represents an interesting future development.

References

[1] D.N. Arnold, F. Brezzi, B. Cockburn, L.D. Marini, Unified analysis of discontinuous Galerkin methods for elliptic problems, SIAM J. Numer. Anal. 39 (2002) 1749–1779.

[2] D.N. Arnold, F. Brezzi, L.D. Marini, A family of discontinuous Galerkin finite elements for the Reissner–Mindlin plate, J. Sci. Comput. 22 (1) (2005) 25–45.

[3] D.N. Arnold, R.S. Falk, A uniformly accurate finite element method for the Reissner–Mindlin plate, SIAM J. Numer. Anal. 26 (1989) 1276–1290.

[4] F. Brezzi, K.J. Bathe, M. Fortin, Mixed-interpolated elements for Reissner–Mindlin plates, Internat. J. Numer. Methods Eng. 28 (1989) 1787–1801.

[5] F. Brezzi, M. Fortin, Mixed and Hybrid Finite Element Methods, Springer, NY, 1991.
[6] F. Brezzi, L.D. Marini, A nonconforming element for the Reissner–Mindlin plate, Comput. & Structures 81 (2003) 515–522.
[7] Z.Q. Cheng, R.C. Batra, Three-dimensional thermoelastic deformations of a functionally graded elliptic plate, Composites Part B 31 (2000) 97–106.
[8] C. Chinosi, C. Lovadina, L.D. Marini, Nonconforming finite elements for Reissner–Mindlin plates, in: M. Primicerio, R. Spigler, V. Valente (Eds.), Applied and Industrial Mathematics in Italy, Series on Advances in Mathematics for Applied Sciences, vol. 69, World Scientific, Singapore, 2005, pp. 213–224.
[9] C. Chinosi, C. Lovadina, L.D. Marini, Nonconforming locking-free finite elements for Reissner–Mindlin plates, Comput. Methods Appl. Mech. Eng. 195 (25–28) (2006) 3448–3460.
[10] L. Della Croce, P. Venini, Finite elements for functionally graded Reissner–Mindlin plates, Comput. Methods Appl. Mech. Eng. 193 (2004) 705–725.
[11] F. Erdogan, Fracture mechanics of functionally graded materials, Composites Eng. 5 (1995) 753–770.
[12] J.H. Jin, R.C. Batra, Some basic fracture mechanics concepts in functionally graded materials, J. Mech. Phys. Solids 44 (1996) 1221–1235.
[13] J.H. Kim, G.H. Paulino, Finite element evaluation of mixed-mode stress intensity factor in functionally graded materials, Internat. J. Numer. Methods Eng. 53 (8) (2002) 1903–1935.
[14] M. Koizumi, The concept of FGM, Ceram. Trans. Funct. Graded Mater. 34 (1993) 3–10.
[15] C. Lovadina, A low-order nonconforming finite element for Reissner–Mindlin plates, SIAM J. Numer. Anal. 42 (2005) 2688–2705.
[16] R.D. Mindlin, Influence of rotary inertia and shear on flexural motion of isotropic elastic plates, J. Appl. Mech. 18 (1951) 31–38.
[17] G.N. Praveen, J.N. Reddy, Nonlinear transient thermoelastic analysis of functionally graded ceramic-metal plates, Internat. J. Solids Structures 35 (1998) 4457–4476.
[18] J.N. Reddy, Analysis of functionally graded plates, Internat. J. Numer. Methods Eng. 47 (2000) 663–684.
[19] J.N. Reddy, C.D. Chin, Thermomechanical analysis of functionally graded cylinders and plates, J. Thermal Stresses 26 (1) (1998) 93–126.
[20] E. Reissner, The effect of transverse shear deformation on the bending of elastic plates, J. Appl. Mech. 23 (1945) 69–77.
[21] S. Suresh, A. Mortensen, Fundamentals of Functionally Graded Materials, Barnes and Noble Publications, 1998
[22] K. Tanaka, Y. Tanaka, H. Watanabe, V.F. Poterasu, Y. Sugano, An improved solution to thermoelastic materials designed in functionally graded materials: scheme to reduce thermal stresses, Comput. Methods Appl. Mech. Eng. 106 (1993) 377–389.
[23] J. Woo, S.A. Meguid, Nonlinear analysis of functionally graded plates and shallow shells, Internat. J. Solids Structures 38 (2001) 7409–7421.